The Generalized Quasilinear Approximation: Application to Zonal Jets

J. B. Marston,[1, *] G. P. Chini,[2, †] and S. M. Tobias[3, ‡]

[1]*Department of Physics, Box 1843, Brown University, Providence, RI 02912-1843, USA*
[2]*Department of Mechanical Engineering & Program in Integrated Applied Mathematics,*
University of New Hampshire, Durham, NH 03824, USA
[3]*Department of Applied Mathematics, University of Leeds, Leeds, LS29JT, U.K.*
(Dated: April 29, 2016)

Quasilinear theory is often utilized to approximate the dynamics of fluids exhibiting significant interactions between mean flows and eddies. We present a generalization of quasilinear theory to include dynamic mode interactions on the large scales. This generalized quasilinear (GQL) approximation is achieved by separating the state variables into large and small zonal scales via a spectral filter rather than by a decomposition into a formal mean and fluctuations. Nonlinear interactions involving only small zonal scales are then removed. The approximation is conservative and allows for scattering of energy between small-scale modes via the large scale (through non-local spectral interactions). We evaluate GQL for the paradigmatic problems of the driving of large-scale jets on a spherical surface and on the β-plane and show that it is accurate even for a small number of large-scale modes. As GQL is formally linear in the small zonal scales it allows for the closure of the system and can be utilized in direct statistical simulation schemes that have proved an attractive alternative to direct numerical simulation for many geophysical and astrophysical problems.

Even with the advent of peta- and exascale computing, many problems of nonlinear physics are not amenable to direct numerical simulations (DNS) of the governing partial differential equations (PDEs) in the parameter regimes of physical relevance. For example, geophysical and astrophysical flows exhibit variability over such a vast range of spatial and temporal scales that DNS of the master PDEs will remain out of reach for the foreseeable future. A number of complementary approaches to DNS have therefore been investigated that employ approximations of varying complexity. These approaches generally attempt to achieve some degree of fidelity for the evolution of the large spatial scales, whilst parameterizing the small-scale interactions in a *sub-grid* model [1]. Typically, the models are constructed by postulating an *ad hoc*, though usually plausible, prescription for the response of the large scales to the small-scale interactions in the form of transport coefficients.

A more robust approach is to construct *self-consistent* equations for the evolution of the low-order statistics of the flow. Termed Direct Statistical Simulation (DSS), this technique has been shown to be able to reproduce mean flows and two-point correlation functions for model problems describing a wide range of physical processes. In its simplest form DSS employs a quasilinear (QL) approximation to describe the interaction between the large and small scales [2–4]. The QL approximation has a long history, owing to its utility in the derivation of analytical theories for turbulent interactions and interactions between waves and mean flows; quasilinear equations often also arise naturally as the result of the asymptotic reduction of a master system of PDEs [5]. This simplest form of DSS has been utilized successfully to describe the statistics of a range of physical systems including the driving of mean flows in plasmas and on giant planets [6], the sustenance of wall-bounded shear-flow turbulence [7], the growth of a dry atmospheric convective boundary layer [8], and even the development of the magnetorotational instability in accretion discs [9].

Although exact in the limit of strong mean flows or for a sufficient separation of timescales [10], DSS truncated at second-order in the nonlocal equal-time cumulant (denoted S3T [2] or CE2 [3]) works less effectively as the system is driven harder, reducing timescale separation with the faster dynamics. This was demonstrated in Ref. 11, which compared the statistics derived from DNS for the problem of driving β-plane jets with those from quasilinear DSS (CE2). CE2 reproduced both the number and strength of jets for large timescale separation but failed as the system was driven further away from equilibrium.

One way to remedy this failure in statistical closures is to employ a higher-order truncation for DSS. This has been pursued by extending the statistical scheme to include eddy/eddy scattering [12]. The resulting schemes (termed CE2.5 or CE3*) have a higher computational cost than those that rely on quasilinear approximations, but *do* perform better as the system is driven further away from equilibrium [12]. Perhaps a better approach is to generalize the QL approximation itself so that it remains amenable to analysis *and* provides a foundation for a new statistical method. Here we evaluate this generalization of QL, which we call GQL, for the important problem of the driving of barotropic jets and demonstrate that it can work even in parameter regimes for which QL (and hence CE2/S3T) will fail. These results motivate a new form of DSS that generalizes the second-order cumulant expansion (GCE2) that we shall demonstrate in a subsequent paper.

Consider modeling the evolution of a state vector $\mathbf{q}(\vec{r}, t)$ specified by a system of master PDEs where (for simplicity) all the nonlinearities in the system are quadratic. This system can be written as

$$\mathbf{q}_t = \mathcal{L}[\mathbf{q}] + \mathcal{N}[\mathbf{q}, \mathbf{q}], \qquad (1)$$

where $\mathcal{L}$ represents a linear vector differential operator and $\mathcal{N}$ is the operator that includes the nonlinear (quadratic) interactions such as those in the material derivative. Specializing to models that are translationally invariant in one direction, denoted the zonal direction, we proceed by generalizing the standard Reynolds decomposition of the state vector into parts, one that oscillates slowly, and one rapidly, in that direction: $\mathbf{q} = \overline{\mathbf{q}} + \mathbf{q}'$. The bandpass filters that we choose are projection operators that obey $\overline{\overline{\mathbf{q}}} = \overline{\mathbf{q}}$ and $\overline{\mathbf{q}'} = 0$ but not $\overline{\overline{\mathbf{q}}\,\mathbf{q}} = \overline{\mathbf{q}}\,\overline{\mathbf{q}}$ as a Reynolds decomposition would. On a rotating sphere, for instance, the filter separates components that oscillate in the azimuthal (ϕ) direction at zonal wavenumbers $|m|$ less than or equal to Λ from those that oscillate with $|m| > \Lambda$:

$$\overline{\mathbf{q}}(\theta, \phi) = \sum_{|m| \leq \Lambda} e^{im\phi}\, \mathbf{q}_m(\theta),$$

$$\mathbf{q}'(\theta, \phi) = \sum_{|m| > \Lambda} e^{im\phi}\, \mathbf{q}_m(\theta). \qquad (2)$$

The GQL approximation is then obtained by neglecting those interactions in the evolution equations represented schematically by Figure 1(d-f); hence

$$\overline{\mathbf{q}}_t \equiv \mathcal{L}[\overline{\mathbf{q}}] + \overline{\mathcal{N}}[\mathbf{q}',\ \mathbf{q}'] + \overline{\mathcal{N}}[\overline{\mathbf{q}},\ \overline{\mathbf{q}}] \qquad (3)$$

$$\mathbf{q}'_t \equiv \mathcal{L}[\mathbf{q}'] + \mathcal{N}'[\overline{\mathbf{q}},\ \mathbf{q}'] + \mathcal{N}'[\mathbf{q}',\ \overline{\mathbf{q}}]\ . \qquad (4)$$

The two nonlinear terms that appear in Eq. 3 correspond to diagrams (a) and (b) in Figure 1 and the sum of the two nonlinear terms in Eq. 4 is interaction (c). Terms $\overline{\mathcal{N}}[\overline{\mathbf{q}},\ \mathbf{q}'] + \overline{\mathcal{N}}[\mathbf{q}',\ \overline{\mathbf{q}}]$ [diagram (d)], $\mathcal{N}'[\overline{\mathbf{q}},\ \overline{\mathbf{q}}]$ [(e)], and $\mathcal{N}'[\mathbf{q}',\ \mathbf{q}']$ [(f)] are discarded. The QL approximation is recovered in the limit $\Lambda = 0$, for which $\overline{\mathbf{q}}$ is simply the zonal mean. In the opposite limit $\Lambda \to \infty$, $\mathbf{q}' = 0$ and the exact and fully nonlinear (NL) dynamics of Eq. 1 are recovered. Thus GQL interpolates between QL and the exact dynamics and provides a systematic way to improve the QL approximation.

An important feature of the new GQL system is that, like QL, the triad interactions that are retained respect the linear and quadratic conservation laws of the original model such as conservation of angular momentum, energy and enstrophy. Two advantages of GQL theory over QL theory should now be emphasized. First, the low modes are allowed to undergo fully nonlinear interactions and thus constitute the resolved model. Satellite modes or zonons therefore can be captured [13]. The second advantage is that small-scale eddies exchange energy through their interaction with the large scales, unlike in
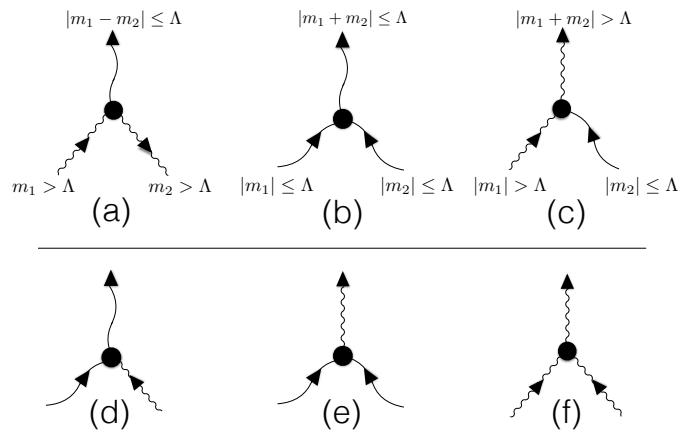

FIG. 1. Triad interactions between modes. Long wavelength fields $\overline{\mathbf{q}}$ with zonal wavenumber $|m| \leq \Lambda$ and short wavelength fields $\mathbf{q}'$ with $|m| > \Lambda$ are shown. Diagrams (a)–(c) in the top row are retained by the GQL approximation and triad interactions (d)–(f) in the bottom row are omitted.

QL in which the mean flow has only zero zonal wavenumber. In GQL energy can be redistributed among smaller zonal scales via scattering off the large-scale flows, a nonlocal spectral transfer. The high modes in the GQL approximation thus function as a novel, deterministic subgrid model. Moreover, GQL is able to predict the responses of the *distributions* for quadratic fluxes (here, Reynolds stresses) in a manner that simply is not possible for QL, since this energy redistribution is *not* captured by a QL (or equivalently, CE2) description.

We examine the effectiveness of the GQL approximation as applied to barotropic dynamics on a spherical surface ($0 \leq \phi < 2\pi$, $0 \leq \theta \leq \pi$) and on a local Cartesian β-plane ($0 \leq x < 2\pi$, $0 \leq y < 2\pi$). The barotropic vorticity equation for $\zeta \equiv \mathbf{e}_1 \cdot (\boldsymbol{\nabla} \times \boldsymbol{u})$, where $\mathbf{e}_1 = \hat{\mathbf{r}}$ on the spherical surface and $\mathbf{e}_1 = \hat{\mathbf{z}}$ on the β-plane, is given by

$$\partial_t \zeta + J(\psi, f + \zeta) = -\kappa\zeta + \mathcal{D} + \eta(t). \qquad (5)$$

Here $J(\ ,\ )$ is the Jacobian and we have utilized the streamfunction representation $\boldsymbol{u} = \boldsymbol{\nabla} \times (\psi\mathbf{e}_1)$. The motion is damped by Rayleigh friction $-\kappa\zeta$ and also a dissipation $\mathcal{D}$ that removes small-scale structures. On the spherical surface $\mathcal{D}$ takes the form of a hyperdiffusion, whilst on the β-plane viscous dissipation $\nu\nabla^2\zeta$ is used. Finally, rotation is incorporated through the Coriolis parameter f, where $f = 2\Omega \cos\theta$ for the spherical system and $f = f_0 + \beta y$ for the local β-plane model. The forcing $\eta(t)$ is chosen to be stochastic and narrow band in spectral space, with a short renewal time [12].

Much is known about the dynamics of this system owing to its importance as a paradigm problem for the formation of jets in Earth's atmosphere and oceans, the outer layers of gas giants, stellar interiors and exoplanets [14–16] and the formation of zonal flows in tokamaks
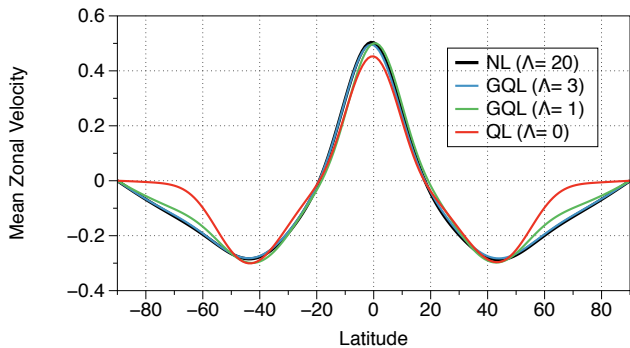
FIG. 2. Time- and zonal-averaged zonal velocity as a function of latitude. Time averaging over 5,000 days (50,000 days for QL) commences after a spin-up of 500 days. NL is the fully nonlinear simulation. In the QL limit ($\Lambda = 0$) there is no mechanism to transfer angular momentum from low latitudes, where it is forced, to high latitudes. GQL corrects this defect.

[5]. Briefly, energy injected at small scales is transferred to larger scales via nonlinear interactions. Owing to the underlying anisotropy of the system, the energy at large scales is preferentially transferred into systematic zonal flows (here a zonal flow is in the ϕ- or x-direction). Two competing mechanisms have been proposed for the energy transport. The first involves the scale-by-scale transfer of energy known as the inverse cascade [17] which involves eddy/eddy scattering. The other is non-local in wavenumber space and relies upon the direct transfer of energy to the largest scales. This forcing via Reynolds stress terms only involves eddies interacting with eddies directly to produce mean flows. Of course in any real fluid system both of these mechanisms are operative, with their relative importance often characterized by the Kubo number R or its analogues [5].

On the sphere, pure spectral DNS with truncation in wavenumbers $0 \leq \ell \leq L$ and $|m| \leq \min\{\ell, M\}$ is performed. We choose spectral cutoffs $L = 30$ and $M = 20$ and work on the unit sphere and in units of time (days) such that $\Omega = 2\pi$. To remove enstrophy cascading to small scales, hyperviscosity $\nu_3(\nabla^2 + 2)\nabla^4 \zeta$ is included. The parameters for the jet are chosen as in Ref. 12. The fluid motion is driven by stochastic forcing η and damped by friction with $\kappa = 0.02$. Only modes with $8 \leq \ell \leq 12$ and $8 \leq |m| \leq \ell$ are stochastically forced. This has the effect of confining the stochastic forcing to lower latitudes. Figure 2 shows that, in contrast with QL, GQL is in fact able to scatter angular momentum to high latitudes, reproducing the zonal flow there as well as at low latitudes. Figure 3 similarly confirms that GQL is able to reproduce the two-point correlation function of the vorticity, again in contrast to QL ($\Lambda = 0$), which shows too strong and too coherent waves owing to the absence of eddy-eddy scattering.

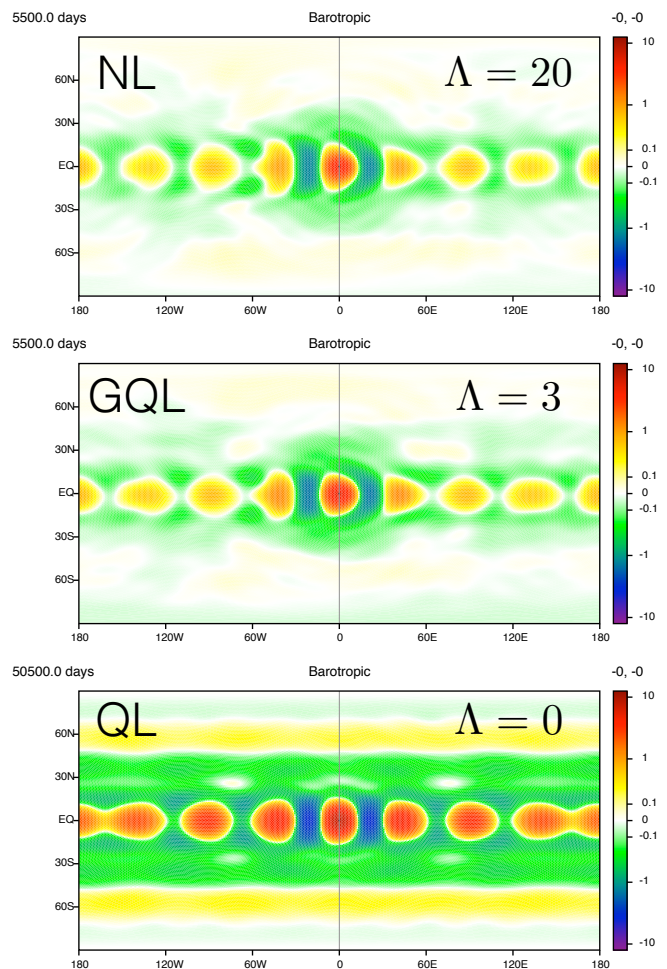Next we evaluate GQL on the β-plane for various

FIG. 3. Second cumulant (two-point correlation function of the vorticity). One point is centered along the prime meridian and at latitude $0°$. The non-local nature of the correlations (or 'teleconnections') is evident.

choices of the cutoff wavenumber Λ. We start by performing a full DNS using a pseudo-spectral scheme [18] at a spectral resolution of 2048^2. As in Ref. [11] the stochastic forcing is chosen to be random but here concentrated in a spectral band of wavenumbers $11 \leq |k_x|, |k_y| \leq 14$. The system is evolved from a state of rest until a solution with 4 strong jets is reached. This state is moderately far from equilibrium as measured by the so-called Zonostrophy Index $R_\beta = 2.6$ [19] and Kubo number $R \approx 0.1$ (the precise values depend on y). It is the subsequent evolution of this state under the various degrees of approximation (different choices of Λ) that we investigate.

Figure 4(a) shows the evolution of the zonal jets as a function of latitude (y) and time (t) in a Hovmöller diagram for the mean vorticity $\bar{\zeta}(y, t)$. At the start of the interval ($t = 0$) 4 jets are visible, but this configuration is unstable and around $t = 4,500$ the two jets nearest the top of the computational domain merge to form one jet. This complicated merging process occurs relatively
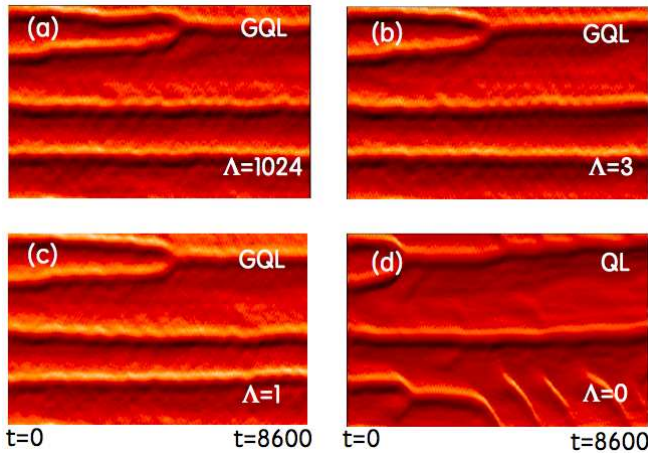
FIG. 4. Color-coded Hovmöller diagram (space-time plots with time t along the horizontal axis and $0 \leq y \leq 2\pi$ along the vertical axis) for the mean vorticity $\overline{\zeta}(y,t)$ for (a) NL DNS ($\Lambda = 1024$), (b) $\Lambda = 3$, (c) $\Lambda = 1$, (d) $\Lambda = 0$ (equivalent to QL).
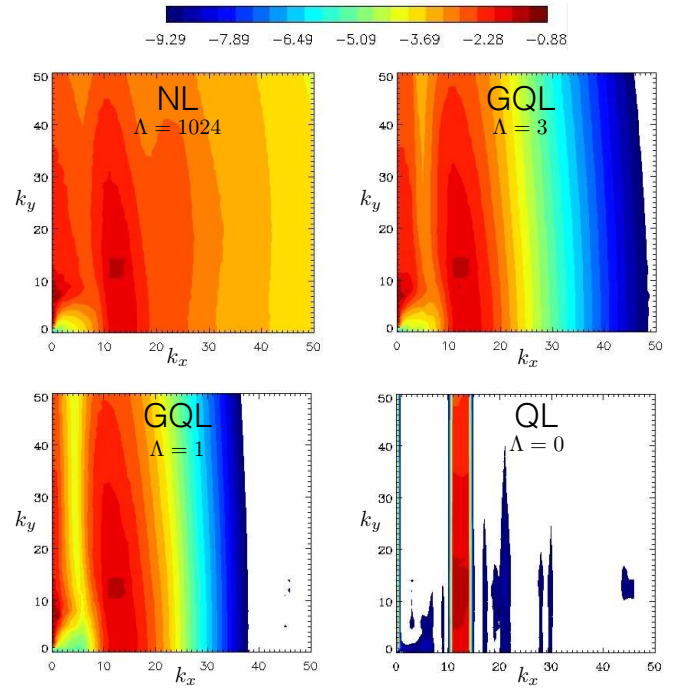

FIG. 5. Time-averaged vorticity power spectra on a $\log_{10}$ scale for fully NL DNS ($\Lambda = 1024$), GQL with $\Lambda = 3$ and $\Lambda = 1$, and QL ($\Lambda = 0$). In all cases power scatters in the meridional y-direction via the nonlinear interaction. Like NL, GQL also redistributes power in the zonal direction. Small power seen in the QL spectrum outside of the forced zonal wavenumbers is due to the initial condition and vanishes rapidly with time.

quickly and the three jet structure remains stable until the end of the computation. Figure 4(b-d) show the comparable evolution in space and time of the mean flow at various levels of truncation. Figure 4(b,c) illustrate the dynamics for $\Lambda = 3$ and $\Lambda = 1$, respectively; for these cases, the forcing injects energy directly into small-scale modes. Remarkably, the GQL approximation run at $\Lambda = 3$ and even $\Lambda = 1$ is able to reproduce the large-scale dynamics of the fully NL DNS. It is only for the quasilinear system ($\Lambda = 0$) that the qualitative dynamics are not replicated; for this case only two jets remain at the end of the run, and the transitions to reach this state are significantly different. The efficacy of the GQL over the QL approximation also may be demonstrated by examining the two-dimensional spectra when averaged over the second half of the evolution. It is clear from Figure 5 that GQL is able to redistribute power over a wide range of zonal wavenumbers.

A formal justification for the GQL approximation is provided by a multiple-scales asymptotic reduction of the PDEs governing a class of anisotropic flows. In the context of the barotropic β-plane vorticity equation (Eq. 5), *two* zonal coordinates and timescales are introduced: $\chi \equiv x$ and $X \equiv \epsilon x$, and $\tau \equiv t$ and $T \equiv \epsilon t$, where ϵ is a scale separation parameter that can be related to the ratio of dissipation to forcing. A *fast-averaging* operation over (χ, τ) is introduced such that each dependent variable is decomposed, in physical space, into a coarse-grained, *slowly-varying* mean field (again denoted with an overbar) and a fluctuation (denoted with a prime): $\zeta(\chi, X, y, \tau, T; \epsilon) = \overline{\zeta}(X, y, T; \epsilon) + \zeta'(\chi, X, y, \tau, T; \epsilon)$. Eq. (5) with multiscale derivatives is parsed into equations for the mean and fluctuation fields, and the vorticity ζ and streamfunction ψ are ex-

panded in asymptotic series in (fractional) powers of ϵ as: $\zeta \sim \overline{\zeta}_0 + \sqrt{\epsilon}\left(\overline{\zeta}_1 + \zeta_1'\right) + \ldots$, and similarly for ψ. The form of these expansions is dictated by the requirements that: (i) the large-scale flow be incompressible; (ii) the (dimensionless) jets $\overline{u} \equiv \partial_y \overline{\psi}$ have $O(1)$ magnitude; and, crucially, (iii) the meridional Reynolds-stress divergence arising from the fluctuation fields feeds back on the slowly-varying mean at the appropriate order. Given these considerations the fluctuation equations are readily deduced to be *quasilinear* about the $O(1)$ mean flow. The equations for the evolution of the slowly-varying mean fields are obtained via a secularity condition, which yields the system

$$\partial_T \overline{\zeta} + J(\overline{\psi}, \overline{\zeta}) + \overline{\beta}\partial_X \overline{\psi} = -\partial_y\left(\overline{\zeta'\partial_\chi \psi'}\right) - \overline{\kappa}\overline{\zeta} + \overline{\mathcal{D}}, \quad (6)$$
$$\partial_y^2 \overline{\psi} = \overline{\zeta}, \quad (7)$$

where $\overline{\beta}$, $\overline{\kappa}$ and $\overline{\mathcal{D}}$ are the $O(1)$ rescaled (dimensionless) beta coefficient, Rayleigh friction coefficient and dissipation, respectively, and the subscripts on the leading-order fields have been omitted. The corresponding leading-order fluctuation system (again dropping subscripts) is given by

$$\partial_\tau \zeta' - \partial_y\overline{\psi}\partial_\chi \zeta' + \partial_\chi \psi'\partial_y\overline{\zeta} + \overline{\beta}\partial_\chi \psi' = \eta'(\tau), \quad (8)$$
$$\left(\partial_\chi^2 + \partial_y^2\right)\psi' = \zeta', \quad (9)$$

where $\eta'(\tau)$ is the fluctuation forcing. Upon reverting to a single set of temporal scales, the GQL formulation can be interpreted as a spectral space implementation of the multiscale reduced PDE system (6)–(9). In the appropriate asymptotic limit, this alternative reduction not only provides a formal mathematical justification for the GQL formulation but also is suggestive of other multiscale algorithms for simulating the reduced dynamics [20].

An extension of quasilinear theory has been introduced for the reduced description of out-of-equilibrium anisotropic fluid systems. GQL theory reinterprets the underlying linearization as the dynamics are linearized about a coarse-grained rather than strictly mean field that undergoes fully nonlinear interactions. One crucial consequence is that energy is redistributed among small-scale modes via scattering off the large-scale flow, in stark contrast to QL dynamics. The utility of GQL theory has been demonstrated for the canonical problem of the driving of zonal jets in barotropic turbulence; for the parameter regime investigated, the accuracy of the QL method is shown to be significantly improved by retaining even just one coarse mode. Further advantages of the method include its ease of implementation and guaranteed preservation of conservation laws of the master equations. The GQL formulation thus provides a seamlessly integrated closure for sub-grid dynamics that has broad applicability to anisotropic turbulent flows arising in nature and technology. Energy redistribution via eddy scattering off the large scales is the key improvement over the QL approximation. The GQL approximation may thus be expected to be widely applicable to systems that include nonlinear interactions between scales – a problem that is ubiquitous in nonlinear physics.

[†] greg.chini@unh.edu
[‡] smt@maths.leeds.ac.uk

[1] B. Fox-Kemper, S. Backman, B. Peason, and S. Reckinger, Clivar Exchanges **19**, 42 (2014).
[2] B. F. Farrell and P. J. Ioannou, J. Atmos. Sci. **64**, 3652 (2007).
[3] J. Marston, E. Conover, and T. Schneider, Journal of the Atmospheric Sciences **65**, 1955 (2008).
[4] K. Srinivasan and W. R. Young, Journal of Atmospheric Sciences **69**, 1633 (2012).
[5] P. H. Diamond, S.-I. Itoh, K. Itoh, and T. S. Hahm, Plasma Phys. Control. Fusion **47**, R35 (2005).
[6] S. M. Tobias, K. Dagon, and J. B. Marston, Astrophys. J. **727**, 127 (2011).
[7] V. L. Thomas, B. F. Farrell, P. J. Ioannou, and D. F. Gayme, Physics of Fluids **27**, 105104 (2015).
[8] F. Ait-Chaalal, T. Schneider, B. Meyer, and J. B. Marston, New Journal of Physics **18**, 025019 (2016).
[9] J. Squire and A. Bhattacharjee, Physical Review Letters **114**, 085002 (2015).
[10] F. Bouchet, C. Nardini, and T. Tangarife, Journal of Statistical Physics **153**, 572 (2013).
[11] S. M. Tobias and J. B. Marston, Phys. Rev. Lett. **110**, 104502 (2013).
[12] J. B. Marston, W. Qi, and S. M. Tobias, (2014), arXiv:1412.0381.
[13] N. A. Bakas and P. J. Ioannou, Physical Review Letters **110**, 224501 (2013).
[14] P. B. Rhines, Journal of Fluid Mechanics **69**, 417 (1975).
[15] G. K. Vallis, *Atmospheric and Oceanic Fluid Dynamics* (Cambridge University Press, 2006).
[16] B. Galperin, S. Sukoriansky, and N. Dikovskaya, Ocean Dynamics **60**, 427 (2010).
[17] G. K. Vallis and M. E. Maltrud, Journal of Physical Oceanography **23**, 1346 (1993).
[18] S. M. Tobias and F. Cattaneo, Journal of Fluid Mechanics **601**, 101 (2008).
[19] B. Galperin, S. Sukoriansky, and N. Dikovskaya, Physica Scripta Volume T **132**, 014034 (2008).
[20] Z. Malecha, G. Chini, and K. Julien, Journal of Computational Physics **271**, 131 (2014).

[*] marston@brown.edu